

This is a repository copy of *First Identification of Excited States in Zr 78 and Implications for Isospin Nonconserving Forces in Nuclei*.

White Rose Research Online URL for this paper:

<https://eprints.whiterose.ac.uk/222802/>

Version: Accepted Version

---

**Article:**

Zimba, G. L., Ruotsalainen, P., Jenkins, D. G. [orcid.org/0000-0001-9895-3341](https://orcid.org/0000-0001-9895-3341) et al. (31 more authors) (2025) First Identification of Excited States in Zr 78 and Implications for Isospin Nonconserving Forces in Nuclei. *Physical Review Letters*. 022502. ISSN 1079-7114

<https://doi.org/10.1103/PhysRevLett.134.022502>

---

**Reuse**

This article is distributed under the terms of the Creative Commons Attribution (CC BY) licence. This licence allows you to distribute, remix, tweak, and build upon the work, even commercially, as long as you credit the authors for the original work. More information and the full terms of the licence here:

<https://creativecommons.org/licenses/>

**Takedown**

If you consider content in White Rose Research Online to be in breach of UK law, please notify us by emailing [eprints@whiterose.ac.uk](mailto:eprints@whiterose.ac.uk) including the URL of the record and the reason for the withdrawal request.

# First identification of excited states in $^{78}\text{Zr}$ and implications for isospin non-conserving forces in nuclei

G. L. Zimba,<sup>1,\*</sup> P. Ruotsalainen,<sup>1</sup> D. G. Jenkins,<sup>2</sup> W. Satuła,<sup>3</sup> J. Uusitalo,<sup>1</sup> R. Wadsworth,<sup>2</sup> X. Pereira Lopez,<sup>4</sup> K. Auranen,<sup>1</sup> A. D. Briscoe,<sup>1,†</sup> B. Cederwall,<sup>5</sup> S. Chen,<sup>2</sup> G. de Angelis,<sup>6</sup> M. Doncel,<sup>7</sup> A. Ertoprak,<sup>5,‡</sup> T. Grahn,<sup>1</sup> P. T. Greenlees,<sup>1</sup> A. Illana,<sup>1,§</sup> H. Joukainen,<sup>1</sup> R. Julin,<sup>1</sup> H. Jutila,<sup>1</sup> J. Keatings,<sup>8</sup> J. Louko,<sup>1</sup> M. Luoma,<sup>1</sup> A. M. Plaza,<sup>1,9</sup> J. Sarén,<sup>1</sup> B. S. Nara Singh,<sup>8</sup> J. Ojala,<sup>1</sup> J. Pakarinen,<sup>1</sup> P. Rahkila,<sup>1</sup> J. Romero,<sup>1,9</sup> J. Sarén,<sup>5</sup> A. Sood,<sup>5</sup> A. Stott,<sup>2</sup> C. Sullivan,<sup>9</sup> H. Tann,<sup>9</sup> A. Tolosa Delgado,<sup>1,¶</sup> and W. Zhang<sup>5</sup>

<sup>1</sup>Accelerator Laboratory, Department of Physics, University of Jyväskylä, FI-40014 Jyväskylä, Finland

<sup>2</sup>School of Physics, Engineering and Technology, University of York, York YO10 5DD, UK

<sup>3</sup>Institute of Theoretical Physics, Faculty of Physics, University of Warsaw, ul. Pasteura 5, PL-02-093 Warsaw, Poland

<sup>4</sup>Center for Exotic Nuclear Studies, Institute for Basic Science (IBS), Daejeon 34126, Republic of Korea.

<sup>5</sup>Department of Physics, KTH Royal Institute of Technology, Stockholm, SE-106 91, Sweden

<sup>6</sup>Istituto Nazionale di Fisica Nucleare, Laboratori Nazionali di Legnaro, Legnaro, I-35020, Italy

<sup>7</sup>Department of Physics, Stockholm University, SE-10691 Stockholm, Sweden

<sup>8</sup>School of Computing Engineering and Physical Sciences, University of the West of Scotland, Paisley PA1 2BE, UK

<sup>9</sup>Department of Physics, Oliver Lodge Laboratory, University of Liverpool, Liverpool, L69 7ZE, United Kingdom

(Dated: October 1, 2024)

At a fundamental level, the interactions between protons and protons, protons and neutrons, and neutrons and neutrons are not identical. Such isospin non-conserving (INC) interactions emerge when comparing the excitation energy of analog states in  $T = 1$  triplet nuclei. Here, we extend such an analysis to the  $A = 78$ ,  $T = 1$  triplet system—the heaviest system for which such complete data exists—and find strong disagreement with contemporary theory. This was achieved by pioneering the technique of recoil- $\beta$ - $\beta$  tagging to identify excited states in  $^{78}\text{Zr}$ . We also established a  $^{78}\text{Zr}$  half-life of  $25_{-8}^{+17}$  ms and extended the  $T = 1$  band in  $^{78}\text{Y}$  to  $J^\pi=(10^+)$ .

Nuclear structure exhibits much complexity and diversity; one of the drivers of this is the fact that the proton and neutron are not identical particles. Trivially, they differ in charge which can manifest as electromagnetic effects in nuclear structure [1]. At a more fundamental level, however, the interactions are not the same between protons and protons, protons and neutrons, and neutrons and neutrons [2, 3]. These differences are attributed to *isospin non-conserving* (INC) interactions where isospin refers to the isospin quantum number,  $T$ , and its projection,  $T_z = (N - Z)/2$ , where  $N$  and  $Z$  are the neutron and proton numbers, respectively [4, 5].

In principle, INC interactions should influence the excitation energy of excited states in all nuclei but it would be near impossible to disentangle such a contribution from all the other aspects of nuclear structure. There do ex-

ist special cases, however, where this is achievable. An example is where the excitation energy of analog  $T = 1$  states is compared across isobaric triplets. The excitation energies should be identical in the absence of INC interactions and a proton/neutron charge difference. The existence of INC interactions is therefore commonly probed by taking the double difference in excitation energies, known as a triplet energy difference, given by

$$\text{TED}(J^\pi) = E_x(J^\pi, T_z = -1) + E_x(J^\pi, T_z = +1) - 2E_x(J^\pi, T_z = 0). \quad (1)$$

where  $E_x(J, T_z)$  are the excitation energies of analog states with spin  $J$  in the three  $T = 1$  triplet nuclei, distinguished by their isospin projection,  $T_z$ . Such TED reflect the difference between the average of the proton-proton and neutron-neutron interactions and the neutron-proton interaction [5, 6].

An open question is whether INC effects are somehow fixed in magnitude across the nuclear chart or whether they exhibit an interplay with other aspects of nuclear structure [7, 8]. In this respect, it would be highly desirable to explore TEDs over a wide mass range and in regions where different nucleon orbitals are expected to dominate. Such an objective is challenging, however, because the balance of nuclear forces means that the relevant  $T = 1$  triplet systems become progressively more exotic as a function of mass. Here, we push our knowledge to the limit by identifying excited states in  $^{78}\text{Zr}$  for

\* zimba@frib.msu.edu; Present address: Facility for Rare Isotope Beams, Michigan State University, MI 48824, USA.

† Present address: Department of Physics, Oliver Lodge Laboratory, University of Liverpool, Liverpool, L69 7ZE, United Kingdom

‡ Present address: Physics Division, Argonne National Laboratory, Lemont, Illinois 60439, USA.

§ Present address: Grupo de Física Nuclear (GFN), EMFTEL, and IPARCOS, Universidad Complutense de Madrid, CEI Moncloa, E-28040 Madrid, Spain

¶ Present address: European Organization for Nuclear Research (CERN), Geneva, Switzerland.

the first time, allowing TEDs for the  $A = 78$ ,  $T = 1$  triplet to be evaluated.

The  $^{40}\text{Ca}(^{40}\text{Ca},2n)$  fusion-evaporation reaction was used to produce  $^{78}\text{Zr}$  at the Accelerator Laboratory of the University of Jyväskylä. A  $^{40}\text{Ca}$  beam with an average intensity of  $3 \times 10^{10}$  ions/s was accelerated to 120 MeV using the K130 cyclotron and bombarded a natural Ca target with approximate thickness of  $0.5 \text{ mg/cm}^2$  for 220 hours. Prompt  $\gamma$  rays were detected using the JUROGAM 3 germanium detector array [9]. The JYUTube scintillator detector array [10], surrounding the target position, was used to select or veto reaction channels associated with charged-particle evaporation. The JYUTube detection efficiency for one proton was approximately 70%. Recoiling nuclei were separated from unreacted beam and other reaction products using a vacuum-mode mass separator called the Mass Analyzing Recoil Apparatus (MARA) [11] and passed through a multi-wire proportional counter (MWPC) to measure recoil position, energy loss, and time-of-flight. The recoils were then implanted in a double-sided silicon strip detector (DSSSD). The DSSSD had active area of  $128.6 \times 48.2 \text{ mm}$  with 192 vertical and 72 horizontal strips [11]. Behind the DSSSD was a segmented plastic scintillator detector called Tuike [12] used to measure the residual energy of  $\beta$  particles that punched through the DSSSD.

In the present work,  $^{78}\text{Zr}$  is expected to be produced with a cross section of order 100 nb or less, which is challenging to discriminate from other strong reaction channels. The approach uniquely adopted in the present work was to correlate  $\gamma$  rays emitted at the target position with recoils detected at the focal plane that decay by the two successive, fast  $\beta$  decays in the decay chain  $^{78}\text{Zr} \rightarrow ^{78}\text{Y} \rightarrow ^{78}\text{Sr}$ . The  $^{78}\text{Y} \rightarrow ^{78}\text{Sr}$  decay is known to be fast with a half-life of  $T_{1/2} = 53(8) \text{ ms}$  [13]. While the half-life of  $^{78}\text{Zr}$  is unknown, it might be anticipated to be of order 20-30 ms, similar to that of  $^{74}\text{Sr}$  (the next lightest even-even  $T_z = -1$  nucleus [14]). Since the  $Q_{EC}$  values for both  $^{78}\text{Zr}$  and  $^{78}\text{Y}$  are expected to be high ( $\approx 10 \text{ MeV}$ ), the energy of detected  $\beta^+$  particles can also be used to discriminate these nuclei from other reaction channels—an approach previously used in the *recoil  $\beta$  tagging* technique [15, 16]. The strategy taken to identify  $^{78}\text{Zr}$  residues therefore relies largely on the characteristic  $\beta$  decays and is presented in Fig. 1. Let us review the event-selection strategy in detail.

First,  $\gamma$  rays and evaporated charged particles are detected at the target position time-prompt with the fusion-evaporation reaction. The recoiling nuclei pass through the MARA recoil separator, with a flight time of  $\sim 1 \mu\text{s}$  and are implanted in a pixel of the DSSSD. A search is then made for two successive  $\beta$  decay events.  $\beta$  decay events in the DSSSD are distinguished from recoil implants by their energy as well as the absence of a coincidence signal in the MWPC. Since the pixels of the DSSSD are relatively small in area ( $\approx 0.45 \text{ mm}^2$ ) and the range of high-energy  $\beta$  particles is substantial in silicon,  $\beta$  particles are also accepted in the analysis if they

are detected in pixels adjacent to the implantation pixel, but excluding the four diagonally adjacent pixels (illustrated in Fig. 1). The correlation search time for the  $^{78}\text{Zr}$  decay was set at 80 ms, approximately three times the estimated half-life of 20-30 ms, and 180 ms for the  $^{78}\text{Y}$  decay, again, approximately three times the known half-life of 53(12) ms. Such decay events were then correlated with recoil events in order to tag the  $\gamma$  rays detected in the JUROGAM 3 array to these specific recoils. In the case that any coincident charged particles were detected in the JYUTube, the recoil event was disregarded.

The final degree of freedom, which can be explored is the residual energy of the  $\beta^+$  particles detected in the Tuike scintillator mounted behind the DSSSD. Figure 2 illustrates the recoil- $\beta$ - $\beta$  tagged  $\gamma$ -ray spectra obtained under the conditions discussed above, and with  $\beta$ -particle energy thresholds of either 2 MeV or 3 MeV applied to both decays. With the former condition, two candidate peaks are seen in the  $\gamma$ -ray spectrum: a peak at 259 keV with six counts and a second peak at 483 keV with three counts. The 259-keV peak on such a sparse background is statistically significant in the  $2\sigma$  limit [17] while the presence of the 483-keV peak is more tentative. The spectrum using a threshold of 3 MeV is cleaner, but both candidate peaks are reduced to two counts (see Fig. 2 (b)). The peaks identified at 259 and 483 keV would appear to be candidates for the  $2^+ \rightarrow 0^+$  and  $4^+ \rightarrow 2^+$  transitions in  $^{78}\text{Zr}$  due to their similar energy to analogous transitions in  $^{78}\text{Y}$  and  $^{78}\text{Sr}$  [18]. Additional confidence in this assignment comes from the fact that the associated recoils best match with the  $A/q$  distribution for  $A = 78$  (see the End Matter).

Having confidently identified events associated with  $^{78}\text{Zr}$ , it is possible to infer its half-life. Figure 3 (a) and (b) show the logarithmic decay time distributions [19, 20] for the first and second  $\beta$  decay, respectively, gated by the 259-keV  $\gamma$  rays. The time difference distribution in Fig. 3 (a) exhibits two well-separated components. A maximum likelihood estimate [19] for the shorter-lived activity associated with the  $\beta$  decay of  $^{78}\text{Zr}$  yields a half-life of  $25_{-8}^{+17} \text{ ms}$ . Similarly, in Fig. 3 (b), the shorter-lived activity, corresponding to the  $\beta$  decay of  $^{78}\text{Y}$ , has an estimated half-life of  $42_{-13}^{+29} \text{ ms}$ , in agreement with the adopted  $^{78}\text{Y}$  ground-state  $\beta$ -decay half-life of 53(8) ms.

The present data also affords additional spectroscopic information on  $^{78}\text{Y}$  populated via the  $^{40}\text{Ca}(^{40}\text{Ca},\text{pn})^{78}\text{Y}$  reaction. This channel can be discriminated using more conventional recoil- $\beta$  tagging [16] combined with a requirement that one charged particle is detected in the JYUTube. Such an analysis confirms the earlier identification of the 281-keV ( $2^+ \rightarrow 0^+$ ) and 505-keV ( $4^+ \rightarrow 2^+$ ) transitions in  $^{78}\text{Y}$  [21]. Higher statistics in the present work reveals further  $\gamma$  rays in coincidence with these two transitions (see Fig. 4 (a)). In particular, a 715-keV  $\gamma$  ray is observed which seems the best candidate for the  $6^+ \rightarrow 4^+$  transition in  $^{78}\text{Y}$ , superseding a previously suggested candidate of 615 keV [21] which is not observed in the present work. Figure 4 (c) shows evidence for 898

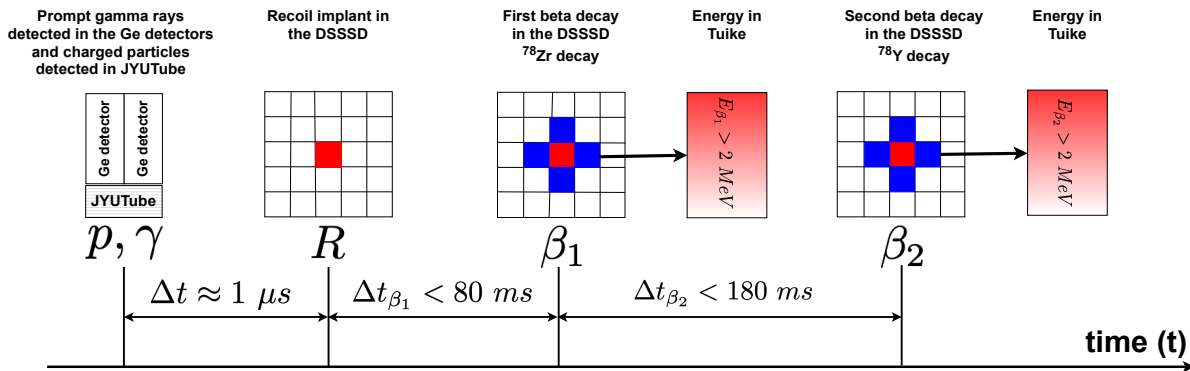


FIG. 1. A schematic of the recoil- $\beta_1 - \beta_2$  correlation technique with a timeline from left to right. The exotic nucleus of interest is produced in a fusion-evaporation reaction; prompt  $\gamma$  rays and evaporated charged particles (if any) are detected at the target position. The nucleus is transported through a recoil separator and is implanted in a DSSSD pixel following a typical flight time of  $1 \mu\text{s}$ . The nucleus then decays by two successive fast  $\beta$  decays within a time period of three times the respective half-lives. Some fraction of  $\beta$  decay events lead to a high-energy  $\beta$  particle depositing some of its energy in the same (or neighbouring) pixel of the DSSSD and the residue of its energy in a plastic scintillator detector mounted behind the DSSSD.

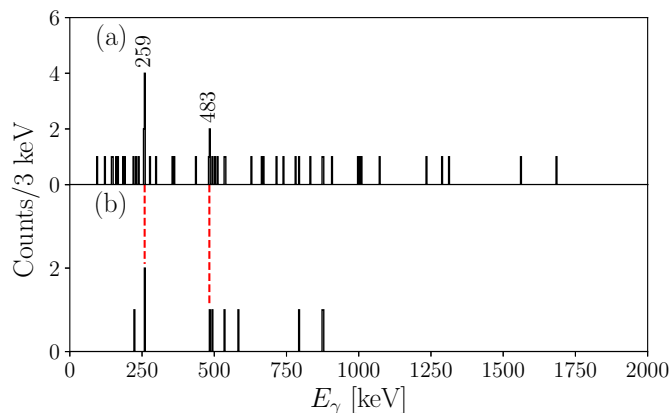


FIG. 2. Recoil- $\beta_1$ - $\beta_2$  correlated  $\gamma$ -ray spectra with correlation search times of 80 ms and 180 ms for the first and second decays, respectively, and  $\beta$ -particle energy thresholds of (a) 2 MeV, and (b) 3 MeV. Only recoils with zero charged particles detected in JYUTube are correlated.

keV and 1062 keV  $\gamma$  rays as tentative candidates for the  $8^+ \rightarrow 6^+$  and  $10^+ \rightarrow 8^+$  transitions in  $^{78}\text{Y}$ , respectively, based on similarity to the respective transition energies in the partner nucleus  $^{78}\text{Sr}$  [18].

Having established one definite and one tentative excited state in  $^{78}\text{Zr}$ , we can evaluate the TED for the  $A = 78$  isobaric triplet (see eq. 1). In addition, the new data allows us to evaluate the mirror energy difference (MED) for the first time, given by

$$\text{MED}(J^\pi) = E_x(J^\pi, T_z = -1) - E_x(J^\pi, T_z = +1). \quad (2)$$

The final permutation available from the excitation energy data is the so-called Coulomb energy difference (CED) given by

$$\text{CED}(J^\pi) = E_x(J^\pi, T_z = 0) - E_x(J^\pi, T_z = +1). \quad (3)$$

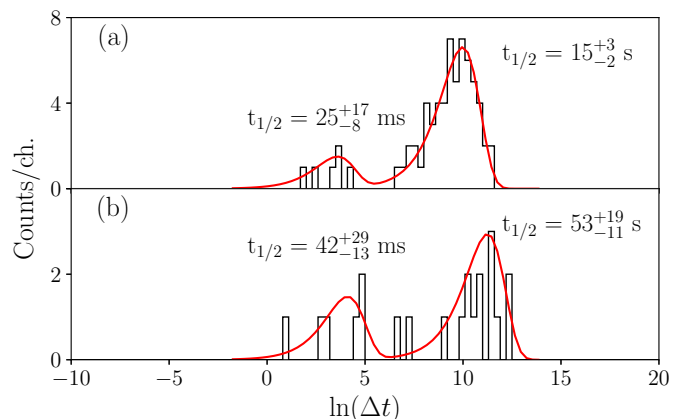


FIG. 3. Natural logarithm of (a)  $\beta_1$ -recoil, and (b)  $\beta_2$ - $\beta_1$  time differences ( $\Delta t$  in milliseconds) gated by the 259-keV  $\gamma$  rays. Recoil- $\beta_1$ - $\beta_2$  correlation conditions are the same as in Fig. 2 (a), but the correlation search time has been extended to 400 s in (a) for  $\beta_1$ , and in (b) for  $\beta_2$  to completely cover the longer-lived components originating from random correlations. The red solid lines show the probability density distributions corresponding to the half-lives obtained from the maximum likelihood estimates.

We are able to extend the earlier more limited CED data for  $A = 78$  based on the new spectroscopic information for  $^{78}\text{Y}$ . The respective TED, CED and MED data are summarised in Fig. 5.

It is challenging in principle for a theoretical model to reproduce the trends of all three of the CED, MED and TED because the contributions to them reflect different aspects of nuclear structure. As elaborated in the introduction, TEDs should emphasise isospin non-conserving interactions (and multipole Coulomb interactions), while CED and MED are sensitive to contributions from monopole Coulomb effects, such as single-

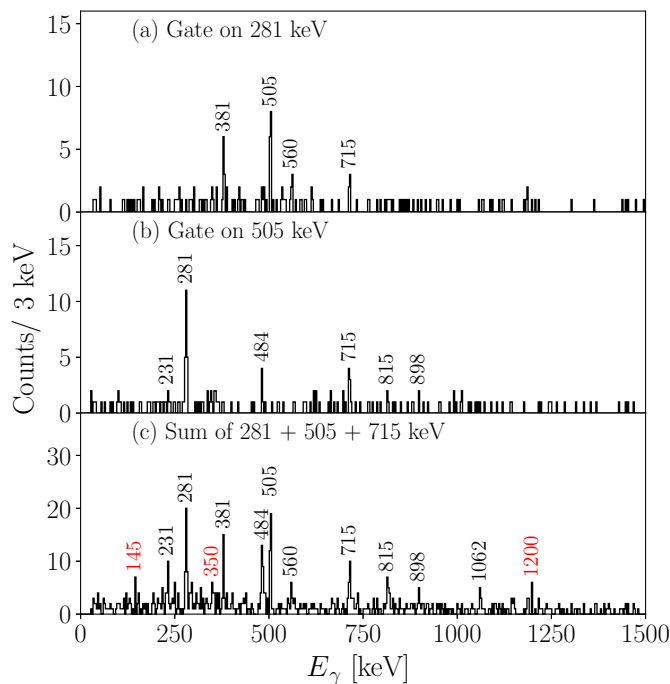


FIG. 4. Recoil- $\beta$  correlated  $\gamma$ - $\gamma$  coincidence spectra gated by the (a) 281-keV, (b) 505-keV, and (c) 281-, 505-, and 715-keV  $\gamma$ -ray transitions in  $^{78}\text{Y}$ . All spectra correspond to detection of one charged particle in JYUTube, and employ a recoil- $\beta$  correlation search time of 150 ms. The  $\beta$ -energy threshold for (a) and (b) was 5 MeV, while for (c) it was 4 MeV. The peak at 145 keV is a contaminant from  $^{77}\text{Rb}$ , while the other peaks labeled in red may originate from  $^{78}\text{Y}$ , but have not been placed in the level scheme of  $^{78}\text{Y}$  (see Fig. 7).

particle Coulomb shifts, changes in nuclear shape or radius, and the electromagnetic spin-orbit interaction.

Over a decade ago, shell-model (SM) calculations using a  $pf_{5/2}g_{9/2}$  model space and the JUN45 interaction [24] predicted CED, MED and TED in the  $A = 78$ ,  $T = 1$  triplet [22]. These predictions do not reproduce the experimental TED and MED extracted in the present work (see Fig. 5 (b) and (c)), but they have been shown to reproduce TED and MED rather well for the  $A = 66$  and  $A = 74$  cases where data already existed [22]. In these latter examples, the trend of TED and MED was to become increasingly negative as a function of spin. Indeed, all known TEDs from  $A = 22$  to  $A = 74$  exhibit such a trend (Fig. 1 of Ref. [22]). The TED for  $A = 78$  follow this systematic trend and do not follow the predictions of the SM calculations [22].

To further understand the discrepancy between the present data and SM predictions, we have carried out calculations based on density functional theory within the no-core-configuration-interaction framework (DFT-NCCI) [23, 25]. This approach is a specific realization of a beyond-mean-field framework designed to study isospin-breaking phenomena in  $N \sim Z$  nuclei [23, 26, 27]. The approach restores rotational symmetry, treats isospin rig-

orously, and mixes states projected from self-consistent mean-field configurations. It is striking that the DFT-NCCI calculations predict TED and MED trends (see Fig. 5) extremely similar to the earlier SM calculations [22]. The CED trend is also highly similar to the SM calculations up to  $J^\pi = 6^+$  and in close agreement with the new experimental data, which extend CEDs up to  $J^\pi = (10^+)$ .

The overall consistency in the SM and DFT-NCCI theoretical approaches is encouraging, but serves only to further highlight the discrepancy with the experimental TED and MED data obtained in the present work. It is striking that all calculated CED, MED and TED for  $A = 78$  are small in magnitude ( $\sim 5$ -10 keV) compared to the other experimentally known triplets. This “quenching” of the energy differences might be expected since the  $A = 78$  nuclei are strongly deformed [28]; indeed, there is a large shell gap at  $N = Z = 38$  in the deformed Nilsson model picture.

It appears that both theoretical models encounter problems in capturing the dynamics of isospin-symmetry breaking (ISB) effects along the rotational band in  $^{78}\text{Zr}$ , which is what gives rise to the large negative MED and TED seen experimentally. This is somewhat unexpected since (i) such effects already appear at the relatively low spins of  $2^+$  and  $4^+$  as compared with the neighboring  $T = 1/2$  mirror pair  $^{79}\text{Zr}/^{79}\text{Y}$  where the MED changes sign at  $\frac{11}{2}^+$  (see Ref. [29]) and (ii) no signature of enhancement in ISB dynamics is visible in the CED. Moreover, the DFT-NCCI calculations predict excitation energies for states in  $^{78}\text{Sr}$  which are in relatively good agreement with that seen experimentally, although the theory does overestimate the moment of inertia, particularly at the lowest spins, which may suggest problems with the theoretical description of pairing correlations, particularly subtleties related to the varying proximity of the continuum across the three members of the triplet.

In summary, we have pioneered the technique of recoil- $\beta$ - $\beta$  tagging and used it to identify a  $2^+$  state (and tentatively a  $4^+$  state) in  $^{78}\text{Zr}$  for the first time. The analysis also determines a half-life of  $25_{-8}^{+17}$  ms for  $^{78}\text{Zr}$ , which is in line with systematics. Several new  $\gamma$ -ray transitions have been observed in  $^{78}\text{Y}$ , where the  $T = 1$  band has been extended to  $J^\pi = (10^+)$ . While the trend in experimental CED for  $A = 78$  is well reproduced by theory, there is a strong discrepancy between experimental MED and TED data, and the SM and DFT-NCCI calculations considered in the present work. The origin of this discrepancy is so far unclear and suggests that further theoretical (and experimental) work in this area is warranted.

The authors acknowledge the GAMMAPOOL European Spectroscopy Resource for the loan of Ge detectors. The authors would also like to express their gratitude to the technical staff of the Accelerator Laboratory at the University of Jyväskylä for their support, especially J. Jaatinen for manufacturing the Ca targets. W. Satula acknowledges the support of the Pol-

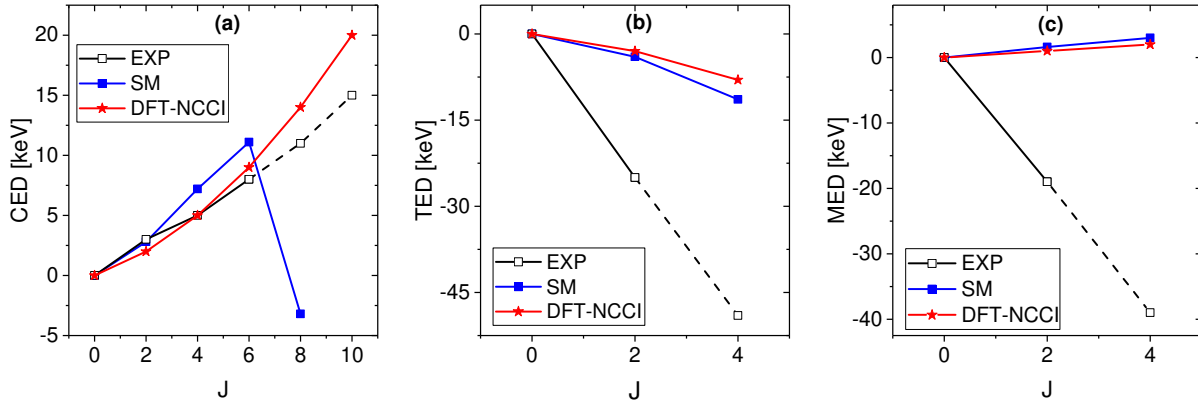


FIG. 5. Comparison of experimentally-derived CED (a), TED (b), and MED (c) as a function of spin ( $J$ ) for the  $A = 78$  triplet with the results of published shell model (SM) calculations [22] and DFT-NCCI calculations carried out in the present work [23]. The solid black lines connect to  $T = 1$  states with confirmed spin-parities, while the dashed black lines connect to tentatively assigned  $T = 1$  states.

ish National Science Centre (NCN) under Contract No 2018/31/B/ST2/02220. XPL acknowledges support by the Institute for Basic Science (IBS) of the Republic of Korea under grant IBS-R031-D1. This work was supported by the Science and Technology Facilities Council grant ST/V001035/1. This work was supported by the Swedish Research Council under Grant No. 2019-04880. The experimental data used to produce this article, and the corresponding metadata, are stored in the Finnish national FAIRdata repository and are available from Ref. [30].

## END MATTER

Here, we provide additional data in support of our identification of excited states in  $^{78}\text{Zr}$  as well as further details on the spectroscopy of  $^{78}\text{Y}$  carried out in the present work. We hope that the latter discussion, while less relevant to the main thrust of the present paper, will be an aid to further research on  $^{78}\text{Y}$ .

First, we show that the small subset of candidate  $^{78}\text{Zr}$  events identified in the present work are convincingly associated with recoils with  $A = 78$ . Figure 6 shows the mass-to-charge-state ( $A/q$ ) distributions of various reaction products measured at the MARA focal plane separated by mass. In order to generate the  $A = 76$  and  $A = 77$  distributions shown in Fig. 6 (a) and (b), we select recoil events correlated with well-established prompt  $\gamma$  rays in  $^{76}\text{Kr}$  and  $^{77}\text{Rb}$ , respectively. In Fig. 6 (c), recoil- $\beta$  tagged prompt  $\gamma$  rays from  $^{78}\text{Y}$  have been employed to determine the relevant  $A/q$  distribution for  $A = 78$ . The  $A/q$  values of recoils corresponding to recoil- $\beta$ - $\beta$  correlated 259-keV  $\gamma$  rays are indicated as red vertical bars in Fig. 6 (c); these seem to match best with  $A = 78$ .

Turning now to the spectroscopic study of low-lying states in  $^{78}\text{Y}$ , let us first consider what, in general, we

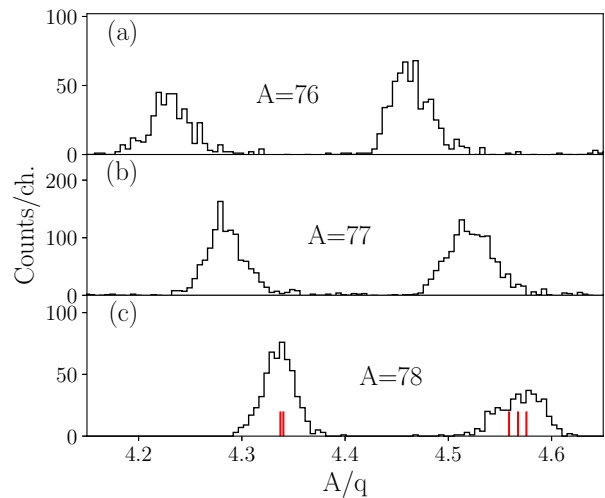


FIG. 6. Measured  $A/q$  distributions at the MARA focal plane for (a)  $^{76}\text{Kr}$ , (b)  $^{77}\text{Rb}$  and (c)  $^{78}\text{Y}$ . The  $A/q$  distributions have been created by gating on the prompt  $\gamma$  rays originating from the respective nuclei. The red vertical bars in panel (c) show the  $A/q$  values of  $\beta$ - $\beta$  correlated recoils gated by 259-keV  $\gamma$  rays.

might expect to see. The first point to note is that odd-odd  $N = Z$  nuclei comprise a special case where the symmetries that apply make the set of possible excited states relatively simple, at least at low excitation energies [31, 32]. Indeed, this is strikingly different to other odd-odd nuclei which typically have a very high level density even close to the ground state, rendering spectroscopic studies highly challenging.

The expectation for an odd-odd  $N = Z$  nucleus such as  $^{78}\text{Y}$  is that it should have two sets of excited states which are interleaved, even at low excitation energy:  $T = 1$  states that should have clear analogues in the other

two members of the  $T = 1$  triplet, and  $T = 0$  states that are isospin-singlet states with no counterpart. These two sets of states should “talk to each other” through  $\gamma$ -ray transitions; indeed, in such odd-odd nuclei, strong isovector  $M1$  transitions are a well-known occurrence [31, 33–35].

Let us provide a reminder of how the spectroscopy of  $^{78}\text{Y}$  was carried out in this case. Here, we employed the technique of recoil- $\beta$  tagging recognising that the half-life of  $^{78}\text{Y}$  is short and the Fermi-Kurie distribution of emitted positrons proceeds to a high  $Q$ -value end point. These two characteristics of the decay may be used for channel selection. In practice, this is achieved by correlating  $\beta$  decays observed both in the DSSSD pixel where the recoil was implanted as well as in the adjacent pixels, excluding the four surrounding diagonal pixels. The recoil- $\beta$  correlation search time was set to 150 ms, corresponding to approximately three times the half-life of the ground state of  $^{78}\text{Y}$ . Typically, the residual energy detected in the Tuik plastic scintillator detector was required to be above 5 MeV. A further requirement in the analysis was the detection of one charged particle in the JYUTube detector corresponding to the  $pn$  evaporation channel leading to  $^{78}\text{Y}$ .

Spectroscopic data for  $^{78}\text{Y}$  including the energy and intensity of  $\gamma$  rays identified in the present work are summarised in Table I. A  $\gamma$ - $\gamma$  coincidence analysis was carried out leading to an extended level scheme for  $^{78}\text{Y}$  shown in Fig. 7. Due to the level of statistics, it was not possible to obtain information on the angular distribution/correlation of  $\gamma$  rays to provide insight into their multipolarity. The approach taken in suggesting assignment for the observed transitions therefore relies on comparison with the known level scheme for  $^{78}\text{Sr}$  for  $T = 1$  states, with the working assumption that transitions/excited states without such obvious counterparts are likely to be associated with a  $T = 0$  state. This latter assumption can only be validated in the future with access to a dataset with significantly higher statistics. Nevertheless, the initial conclusions here are likely to be helpful to such a future analysis and we therefore set them down here. It should be noted that there is a part of the expected level scheme of  $^{78}\text{Y}$  that we cannot see, namely, states built on a previously proposed isomer in  $^{78}\text{Y}$  with suggested spin-parity ( $5^+$ ), half-life of 5.8(6) s and excitation energy  $< 800$  keV [36]. Owing to its long half-life, it is not possible to carry out a recoil- $\beta$  correlation with such an isomer. Given its relatively high spin and low excitation energy, significant flux is likely to reach this isomer and not the ground state, and, hence, be lost to the present analysis.

Having set out the limitations of the present work, let us go on to discuss candidate  $T = 1$  and  $T = 0$  states separately below.

Prior to the present work, candidates for the  $2^+ \rightarrow 0^+$  (281 keV),  $4^+ \rightarrow 2^+$  (505 keV) and  $6^+ \rightarrow 4^+$  (615 keV) transitions in  $^{78}\text{Y}$  had been identified [21]. The present  $\beta$ -tagging analysis independently confirms the assignment

TABLE I. Prompt  $\gamma$ -ray transitions found to be correlated with  $^{78}\text{Y}$  recoils in the present work. Spectroscopic information provided includes the energy of the  $\gamma$  ray ( $E_\gamma$ ), the relative intensity ( $I_{rel}$ ) normalized to the  $2^+ \rightarrow 0^+$  transition, initial level energy ( $E_i$ ) and spin-parity ( $I_i^\pi$ ), and final level energy ( $E_f$ ) and spin-parity ( $I_f^\pi$ ).

$E_\gamma$ [keV]	$I_{rel}$ [%]	$E_i$ [keV]	$E_f$ [keV]	$I_i^\pi$	$I_f^\pi$
230.7(5)	$<10$	1501.1(8)	(1270.1(7))	$6^+$	( $5^+$ )
281.1(4)	100(14)	281.1(4)	0.0	$2^+$	$0^+$
380.8(4)	28(7)	661.9(4)	281.1(4)	( $3^+$ )	$2^+$
484.0(5)	$<10$	(1270.1(7))	786.2(5)	( $5^+$ )	$4^+$
505.0(3)	85(14)	786.2(5)	281.1(4)	$4^+$	$2^+$
559.9(10)	11(4)	841.0(7)	281.1(4)		( $2^+$ )
714.9(5)	21(6)	1501.1(8)	786.2(5)	$6^+$	$4^+$
815.0(10)	$<10$	2316.1(8)	1501.1(8)		$6^+$
898.0(10)	$<10$	2399.1(13)	1501.1(8)	( $8^+$ )	$6^+$
1062.0(10)	$<10$	3461.1(16)	2399.9(13)	( $10^+$ )	( $8^+$ )

of the 281- and 505-keV  $\gamma$  rays but there is no evidence for a 615 keV  $\gamma$  ray in coincidence with the 281 and 505 keV transitions. Instead, a 715 keV  $\gamma$  ray (see Fig. 4 (a) and (b)) forms a clear candidate for the  $6^+ \rightarrow 4^+$  transition. Indeed, the analogous transition in the  $T = 1$  triplet partner,  $^{78}\text{Sr}$ , has an energy of 712 keV [18].

Due to the level of statistics, it becomes challenging to identify higher spin states in the  $T = 1$  band and we have to rely more heavily on comparison with the isobaric triplet partner,  $^{78}\text{Sr}$ . In this respect, we identify a candidate  $8^+ \rightarrow 6^+$  transition with an energy of 898 keV (see Fig. 4 (b) and (c)) which is close in energy to the corresponding 895 keV transition in  $^{78}\text{Sr}$ . Similarly, a 1062 keV transition is candidate for the  $10^+ \rightarrow 8^+$  transition based on close similarity to the 1058-keV transition in  $^{78}\text{Sr}$  (see Fig. 4 (c)). Given the level of statistics, we treat the assignment of the 898 and 1062 keV transitions as tentative.

Knowledge of low-lying non-yrast states in  $^{78}\text{Sr}$  is somewhat limited and so it is not possible to make further useful comparisons to find additional  $T = 1$  states. On this basis, we assume that the additional  $\gamma$ -ray transitions identified in the present work connect to  $T = 0$  states, but this is not guaranteed.

A newly observed  $\gamma$  ray with an energy of 381 keV (see Fig. 4 (a)) has been assigned as de-exciting a state feeding the  $2^+$  state in the  $T = 1$  band in  $^{78}\text{Y}$ . Given the relative strength of this transition and the expected dominance of isovector  $M1$  transitions, we might propose ( $3^+$ ) for the state which it de-excites.

The 560-keV  $\gamma$  ray, although previously observed [28], was not assigned as de-exciting a state feeding any states in  $^{78}\text{Y}$ . In the present analysis, the 560-keV  $\gamma$  ray is assigned as de-exciting a state feeding the  $2^+$  state in the  $T = 1$  band from a state with an energy of 841 keV.

The 231- and 484-keV  $\gamma$  rays observed in Fig. 4 (b) and (c) are suggested to comprise an alternate decay path connecting the  $6^+$  and  $4^+$  states in the  $T = 1$  band in  $^{78}\text{Y}$ . This assignment is based on considering their rela-

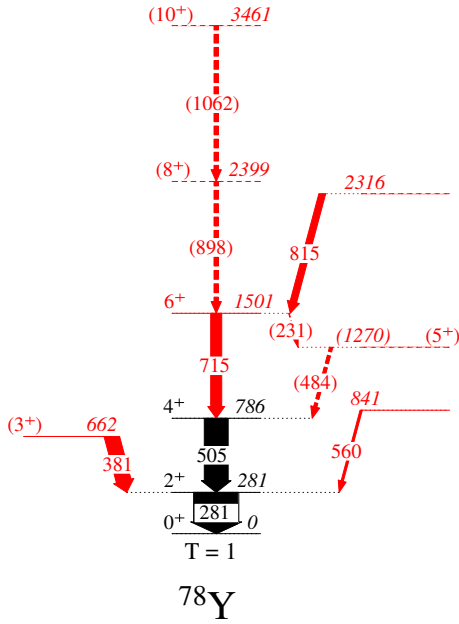


FIG. 7. A partial level scheme for  $^{78}\text{Y}$  deduced in the present work. The width of the arrows are proportional to the intensity of the transition. The intensities of the  $\gamma$ -ray transitions are extracted from the recoil- $\beta$ -tagged  $\gamma$  singles or  $\gamma$ - $\gamma$  coincidence data. Newly assigned levels and  $\gamma$ -ray transitions are labelled in red. Previously observed transitions in Ref. [28], which were also observed in the present work, are labeled in black. Tentatively assigned transitions are shown as dashed lines.

tive intensities and noting that their energies sum to the energy difference between the  $6^+$  and  $4^+$  states. On this basis, and, again, expecting to observe strong isovector  $M1$  transitions, we propose the state between these two transitions has  $J^\pi = (5^+)$ . An 815-keV  $\gamma$  ray is observed in coincidence with the 505-keV  $\gamma$ -ray as shown in Fig. 4 (b). Coincidence analysis suggests that this  $\gamma$  ray feeds the  $T = 1$ ,  $6^+$  state at 1501 keV from a state with an energy of 2316 keV.

- 
- [1] G. A. Miller, A. K. Opper, and E. J. Stephenson, *Annu Rev. Nucl. Part. Sci.* **56**, 253 (2006).
- [2] E. M. Henley, *Isospin in Nuclear Physics* (North Holland Publishing, Amsterdam, 1969).
- [3] P. E. Garrett, W. E. Ormand, D. Appelbe, R. W. Bauer, J. A. Becker, L. A. Bernstein, J. A. Cameron, M. P. Carpenter, R. V. F. Janssens, C. J. Lister, D. Seweryniak, E. Tavukcu, and D. D. Warner, *Phys. Rev. Lett.* **87**, 132502 (2001).
- [4] E. Wigner, *Phys. Rev.* **51**, 106 (1937).
- [5] M. Bentley and S. Lenzi, *Prog. Part. Nucl. Phys.* **59**, 497 (2007).
- [6] M. A. Bentley, S. M. Lenzi, S. A. Simpson, and C. A. Diget, *Phys. Rev. C* **92**, 024310 (2015).
- [7] G. L. Zimba, P. Ruotsalainen, G. De Gregorio, G. de Angelis, J. Sarén, J. Uusitalo, K. Auranen, A. D. Briscoe, Z. Ge, T. Grahn, P. T. Greenlees, A. Illana, D. G. Jenkins, H. Joukainen, R. Julin, H. Jutila, A. Kankainen, J. Louko, M. Luoma, J. Ojala, J. Pakarinen, A. Raggio, P. Rahkila, J. Romero, M. Stryjczyk, A. Tolosa-Delgado, R. Wadsworth, and A. Zadvornaya, *Phys. Rev. C* **110**, 024314 (2024).
- [8] D. M. Debenham, M. A. Bentley, P. J. Davies, T. Haylett, D. G. Jenkins, P. Joshi, L. F. Sinclair, R. Wadsworth, P. Ruotsalainen, J. Henderson, K. Kaneko, K. Auranen, H. Badran, T. Grahn, P. Greenlees, A. Herzañ, U. Jakobsson, J. Konki, R. Julin, S. Juutinen, M. Leino, J. Sorri, J. Pakarinen, P. Papadakis, P. Peura, J. Partanen, P. Rahkila, M. Sandzelius, J. Sarén, C. Scholey, S. Stolze, J. Uusitalo, H. M. David, G. de Angelis, W. Korten, G. Lotay, M. Mallaburn, and E. Sahin, *Phys. Rev. C* **94**, 054311 (2016).
- [9] J. Pakarinen, J. Ojala, P. Ruotsalainen, H. Tann, H. Badran, T. Calverley, J. Hilton, T. Grahn, P. T. Greenlees, M. Hytönen, A. Illana, A. Kauppinen, M. Luoma, P. Papadakis, J. Partanen, K. Porras, M. Puskala, P. Rahkila, K. Ranttila, J. Sarén, M. Sandzelius, S. Szewc, J. Tuunanen, J. Uusitalo, and G. Zimba, *Eur. Phys. J. A*, **56**, 149 (2010).
- [10] G. L. Zimba, *Spectroscopy along the  $N = Z$  line between mass 70 and 84*, *Ph.D. thesis*, Department of Physics, University of Jyväskylä (2023).
- [11] J. Uusitalo, J. Saren, J. Partanen, and J. Hilton, *Acta Phys. Pol. B* **50**, 319 (2019).
- [12] H. Joukainen, J. Sarén, and P. Ruotsalainen, *Nucl. Instr. and Meth. A* **1027**, 166253 (2022).

- [13] A. R. Farhan and B. Singh, *Nucl. Data Sheets* **110**, 1917 (2009).
- [14] L. Sinclair, R. Wadsworth, J. Dobaczewski, A. Pastore, G. Lorusso, H. Suzuki, D. S. Ahn, H. Baba, F. Browne, P. J. Davies, P. Doornenbal, A. Estrade, Y. Fang, N. Fukuda, J. Henderson, T. Isobe, D. G. Jenkins, S. Kubono, Z. Li, D. Lubos, S. Nishimura, I. Nishizuka, Z. Patel, S. Rice, H. Sakurai, Y. Shimizu, P. Schury, H. Takeda, P.-A. Söderström, T. Sumikama, H. Watanabe, V. Werner, J. Wu, and Z. Y. Xu, *Phys. Rev. C* **100**, 044311 (2019).
- [15] A. Steer, D. Jenkins, R. Glover, B. Nara Singh, N. Pattabiraman, R. Wadsworth, S. Eeckhaudt, T. Grahn, P. Greenlees, P. Jones, R. Julin, S. Juutinen, M. Leino, M. Nyman, J. Pakarinen, P. Rahkila, J. Sarén, C. Scholey, J. Sorri, J. Uusitalo, P. Butler, I. Darby, R.-D. Herzberg, D. Joss, R. Page, J. Thomson, R. Lemmon, J. Simpson, and B. Blank, *Nucl. Instr. and Meth. A* **565**, 630 (2006).
- [16] J. Henderson, P. Ruotsalainen, D. G. Jenkins, C. Scholey, K. Auranen, P. J. Davies, T. Grahn, P. T. Greenlees, T. W. Henry, A. Herzán, U. Jakobsson, P. Joshi, R. Julin, S. Juutinen, J. Konki, M. Leino, G. Lotay, A. J. Nichols, A. Obertelli, J. Pakarinen, J. Partanen, P. Peura, P. Rahkila, M. Sandzelius, J. Sarén, J. Sorri, S. Stolze, J. Uusitalo, and R. Wadsworth, *JINST* **8**, P04025 (2013).
- [17] G. J. Feldman and R. D. Cousins, *Phys. Rev. D* **57**, 3873 (1998).
- [18] D. Rudolph, C. Baktash, C. J. Gross, W. Satula, R. Wyss, I. Birriel, M. Devlin, H.-Q. Jin, D. R. LaFosse, F. Lerma, J. X. Saladin, D. G. Sarantites, G. N. Sylvan, S. L. Tabor, D. F. Winchell, V. Q. Wood, and C. H. Yu, *Phys. Rev. C* **56**, 98 (1997).
- [19] K. H. Schmidt, C. C. Sahm, K. Pielenz, and H. G. Clerc, *Z Phys. A* **316**, 19 (1984).
- [20] K. H. Schmidt, *Eur. Phys. J. A* **8**, 141 (2000).
- [21] B. S. Nara Singh, A. N. Steer, D. G. Jenkins, R. Wadsworth, M. A. Bentley, P. J. Davies, R. Glover, N. S. Pattabiraman, C. J. Lister, T. Grahn, P. T. Greenlees, P. Jones, R. Julin, S. Juutinen, M. Leino, M. Nyman, J. Pakarinen, P. Rahkila, J. Sarén, C. Scholey, J. Sorri, J. Uusitalo, P. A. Butler, M. Dimmock, D. T. Joss, J. Thomson, B. Cederwall, B. Hadinia, and M. Sandzelius, *Phys. Rev. C* **75**, 061301 (2007).
- [22] K. Kaneko, Y. Sun, T. Mizusaki, and S. Tazaki, *Phys. Rev. C* **89**, 031302 (2014).
- [23] W. Satuła, P. Bączyk, J. Dobaczewski, and M. Konieczka, *Phys. Rev. C* **94**, 024306 (2016).
- [24] M. Honma, T. Otsuka, T. Mizusaki, and M. Hjorth-Jensen, *Phys. Rev. C* **80**, 064323 (2009).
- [25] See Supplemental Material at [URL will be inserted by publisher], for further details on the NCCI calculations, the procedure followed and the configurations used.
- [26] P. Bączyk, J. Dobaczewski, M. Konieczka, W. Satuła, T. Nakatsukasa, and K. Sato, *Phys. Lett. B* **778**, 178 (2018).
- [27] P. Bączyk, W. Satuła, J. Dobaczewski, and M. Konieczka, *J. Phys. G: Nucl. Part. Phys.* **46**, 03LT01 (2019).
- [28] R. D. O. Llewellyn, M. A. Bentley, R. Wadsworth, H. Iwasaki, J. Dobaczewski, G. de Angelis, J. Ash, D. Bazin, P. C. Bender, B. Cederwall, B. P. Crider, M. Doncel, R. Elder, B. Elman, A. Gade, M. Grinder, T. Haylett, D. G. Jenkins, I. Y. Lee, B. Longfellow, E. Lunderberg, T. Mijatović, S. A. Milne, D. Muir, A. Pastore, D. Rhodes, and D. Weisshaar, *Phys. Rev. Lett.* **124**, 152501 (2020).
- [29] R. D. O. Llewellyn, M. A. Bentley, R. Wadsworth, J. Dobaczewski, W. Satuła, H. Iwasaki, G. de Angelis, J. Ash, D. Bazin, P. C. Bender, B. Cederwall, B. P. Crider, M. Doncel, R. Elder, B. Elman, A. Gade, M. Grinder, T. Haylett, D. G. Jenkins, I. Y. Lee, B. Longfellow, E. Lunderberg, T. Mijatović, S. A. Milne, D. Rhodes, and D. Weisshaar, *Phys. Lett. B* **811**, 135873 (2020).
- [30] K. Auranen, A. Briscoe, B. Cederwall, G. de Angelis, M. Doncel, A. Ertoprak, T. Grahn, P. T. Greenlees, A. Ilana, D. G. Jenkins, H. Joukainen, R. Julin, H. Jutila, J. Keatings, J. Louko, M. Luoma, A. Montes, B. S. N. Singh, J. Ojala, J. Pakarinen, J. P. Lopez, P. Rahkila, J. Romero, P. Ruotsalainen, J. Sarén, C. Sidong, A. Sood, A. Stott, C. Sullivan, H. Tann, A. T. Delgado, J. Uusitalo, R. Wadsworth, Z. Wei, and G. Zimba, *Fairdata.fi* (2024), <https://doi.org/10.23729/543400fe-5581-4641-89f6-874cca17efb7>.
- [31] D. G. Jenkins, N. S. Kelsall, C. J. Lister, D. P. Balamuth, M. P. Carpenter, T. A. Sienko, S. M. Fischer, R. M. Clark, P. Fallon, A. Görgen, A. O. Macchiavelli, C. E. Svensson, R. Wadsworth, W. Reviol, D. G. Sarantites, G. C. Ball, J. Rikovska Stone, O. Juillet, P. Van Isacker, A. V. Afanasjev, and S. Frauendorf, *Phys. Rev. C* **65**, 064307 (2002).
- [32] G. de Angelis, T. Martinez, A. Gadea, N. Marginean, E. Farnea, E. Maglione, S. Lenzi, W. Gelletly, C. A. Ur, D. R. Napoli, T. Kroell, S. Lunardi, B. Rubio, M. Axiotis, D. Bazzacco, A. M. B. Sona, P. G. Bizzeti, P. Bednarczyk, A. Bracco, F. Brandolini, F. Camera, D. Curien, M. D. Poli, O. Dorvaux, J. Eberth, H. Grawe, R. Menegazzo, G. Nardelli, J. Nyberg, P. Pavan, B. Quintana, C. R. Alvarez, P. Spolaore, T. Steinhart, I. Stefanescu, O. Thelen, and R. Venturelli, *Eur. Phys. J. A* **12**, 51 (2001).
- [33] S. M. Lenzi, D. R. Napoli, C. A. Ur, D. Bazzacco, F. Brandolini, J. A. Cameron, E. Caurier, G. de Angelis, M. De Poli, E. Farnea, A. Gadea, S. Hankonen, S. Lunardi, G. Martínez-Pinedo, Z. Podolyak, A. Poves, C. Rossi Alvarez, J. Sánchez-Solano, and H. Somacal, *Phys. Rev. C* **60**, 021303 (1999).
- [34] P. von Brentano, A. Lisetskiy, I. Schneider, C. Frießner, R. Jolos, N. Pietralla, A. Schmidt, and R. Jolos, *Prog. Part. Nucl. Phys.* **44**, 29 (2000).
- [35] N. Pietralla, R. Krücken, C. J. Barton, C. W. Beausang, M. A. Caprio, R. F. Casten, J. R. Cooper, A. A. Hecht, J. R. Novak, N. V. Zamfir, A. Lisetskiy, and A. Schmidt, *Phys. Rev. C* **65**, 024317 (2002).
- [36] J. Uusitalo, D. Seweryniak, P. F. Mantica, J. Rikovska, D. S. Brenner, M. Huhta, J. Greene, J. J. Ressler, B. Tomlin, C. N. Davids, C. J. Lister, and W. B. Walters, *Phys. Rev. C* **57**, 2259 (1998).